

MIT Open Access Articles

Sensitivity of EUV resists to out-of-band radiation

The MIT Faculty has made this article openly available. **Please share** how this access benefits you. Your story matters.

Citation: Roberts, Jeanette M. et al. "Sensitivity of EUV resists to out-of-band radiation." Advances in Resist Materials and Processing Technology XXVI. Ed. Clifford L. Henderson. San Jose, CA, USA: SPIE, 2009. 72731W-13. © 2009 SPIE--The International Society for Optical Engineering

As Published: <http://dx.doi.org/10.1117/12.814342>

Publisher: The International Society for Optical Engineering

Persistent URL: <http://hdl.handle.net/1721.1/52681>

Version: Final published version: final published article, as it appeared in a journal, conference proceedings, or other formally published context

Terms of Use: Article is made available in accordance with the publisher's policy and may be subject to US copyright law. Please refer to the publisher's site for terms of use.



Sensitivity of EUV resists to out-of-band radiation

Jeanette M. Roberts^{*a}, Robert L. Bristol^a, Todd R. Younkin^a, Theodore H. Fedynyshyn^b, David K. Astolfi^b, and Alberto Cabral^b

^aIntel Corporation, Hillsboro, OR 97124

^bLincoln Laboratory, Massachusetts Institute of Technology, Lexington, MA 02420

ABSTRACT

Here we present the relative sensitivity of EUV resists to out of band radiation (OOB), specifically wavelengths in the range 157 - 400 nm. EUV light sources have specifications limiting the allowed energy output in that spectral range yet there is little data supporting the specified values. Filters might be required to meet the spectral purity specifications which will likely have the detrimental effect of reducing the in-band radiation at 13.5 nm and therefore negatively impact the cost of ownership of EUV lithography. To better quantify the effects of OOB we obtained contrast curves and absorbance spectra for several EUV resist platforms at nine exposure wavelengths. The 2007 ITRS Roadmap suggests that resist thicknesses will be near 35 - 65 nm when EUV will be used¹. We found that, in this optically thin regime, resist sensitivity increases with increasing absorbance. The sensitivity decreases dramatically for wavelengths approaching 300 nm, and is negligible for longer wavelengths. The OOB sensitivity of the resists examined can be estimated to within an order of magnitude using the resist absorbance value. For resists with absorbance values on the same order of magnitude, sensitivity is determined by other aspects of the resist formulation. Within the wavelength region explored, the greatest concern is near 160 - 240 nm based on current resist sensitivity characteristics. However, there is a gap in data between 13.5 - 157 nm and there may be other reasons to limit the source output in that wavelength range. The data presented here could be useful in setting or modifying the OOB specifications for EUV tools.

Keywords: Extreme Ultraviolet Lithography, EUVL, Resist, Sensitivity, out-of-band, spectral purity

1. INTRODUCTION

EUV Lithography is being developed as a potential successor to 193 nm lithography for printing the smallest microprocessor features². Resists developed for EUV are typically based on modifications to materials developed for other lithographic exposures, specifically 248 nm, 193 nm, and e-beam³. Therefore, EUV resists are sensitive to radiation other than 13.5 nm, as has been demonstrated⁴⁻⁶. EUV sources produce light over a wide spectral range⁷⁻¹⁰. The multilayer coated (MLC) mirrors used in the optics are effective at narrowing the EUV spectral output to peak at 13.5 nm with a bandwidth of $\pm 2\%$. However, the mirrors also reflect other wavelengths. If OOB light produced by the source reaches the wafer plane, and the resist is sensitive to that light, then contrast will be reduced resulting in degraded imaging performance⁶. The purpose of this study is to characterize the sensitivity of typical EUV resists to OOB radiation. Mbanao et al. measured the sensitivity of 4 resists in the spectral range 190-650 nm⁵. The study presented here extends the spectral range down to 157 nm and includes a wider breadth of resist types with data collected on 13 different materials. Moreover, all resists in this study were 60 nm thick (which is expected to be relevant when EUV is implemented), and bottom anti-reflective coatings (BARCs) were used to reduce the effects of substrate reflection on the clearing dose.

* Jeanette.Roberts@Intel.com

2. EXPERIMENTAL

2.1 Photoresist materials

When selecting materials we strove to cover a wide range of resist platforms and included both fully formulated top-performing proprietary resists as well as published model resists (see Table 1). Seven of the resists selected are provided by commercial suppliers. The specific formulations are not public but they represent a broad range of materials including ones that use 1) polystyrene (PS) type polymers developed for 248 nm lithography - predominately comprised of aromatic monomers such as hydroxystyrene, 2) acrylate type polymers developed for 193 nm lithography, and 3) hybrid polymers useful as one approach to EUVL. This last category includes polymers comprised of both PS type and acrylate type monomers as well as acrylate polymers with EUV (phenolic) sensitizers¹¹. The commercial resists include traditional formulations with the photoacid generator (PAG) blended into the resist as well as resists in which the PAG is anchored to the polymer backbone. Several of the resists have been the leading EUV platform at Intel within the last two years (based on resolution, line-width roughness, and sensitivity), and 3 of the resists have identical formulations except for the base quencher loading level.

Resist Code	Resist Name	Resist Type	PAG	Base Quencher
MODEL RESISTS				
PS(M)-2	LUVR-99497	PHS based	TPS -OTf 5%	1-piperidineethanol 0.2%
PS-Acrylate(M)-3	LUVR-99474	PHS-Acrylate hybrid based	TBPI-PFBS 5%	1-piperidineethanol 0.2%
PS-Acrylate(M)-4	LUVR-99494	PHS-Acrylate hybrid based	TPS -OTf 5%	1-piperidineethanol 0.2%
PS-Acrylate(M)-7	LUVR-99496	PHS-Acrylate hybrid based	TPS -OTf 5%	1-piperidineethanol 0.2%
Acrylate(M)-2	LUVR-99495	Acrylate based	TPS -OTf 5%	1-piperidineethanol 0.2%
F-Acrylate(M)-1	LUVR-99498	Fluoroacrylate based	TPS -OTf 5%	1-piperidineethanol 0.2%
COMMERCIAL RESISTS				
PS(C)-1		PHS based	Proprietary	Proprietary
PS-Acrylate(C)-1		Acrylate based + EUV sensitizer	Proprietary	Proprietary
PS-Acrylate(C)-8		Acrylate based + EUV sensitizer	Proprietary	Proprietary
PS-Acrylate(C)-2		PHS-Acrylate hybrid based	Proprietary	Proprietary X%
PS-Acrylate(C)-5		PHS-Acrylate hybrid based	Proprietary	Same as PS-Acrylate(C)-2 ½ X%
PS-Acrylate(C)-6		PHS-Acrylate hybrid based	Proprietary	Same as PS-Acrylate(C)-2 ⅓ X%
Acrylate(C)-1		Acrylate based	Proprietary	Proprietary

Table 1 –Summary of the resist formulations examined. The PAGs used in the MIT-LL model resists were t-butyl diphenyl iodonium nonaflate (TBPI-PFBS) and triphenyl sulphonium triflate (TPS-OTf).

The model resists also include PS, acrylate, and hybrid PS-acrylate polymers, as well as a fluoropolymer initially developed for 157 nm and 193 nm lithographies. These polymers have been described previously¹²⁻¹⁵ and are presented in Table 2. Typical PAG and base quencher loading levels were used. The base quencher 1-piperidineethanol was added at 0.2 wt % relative to the polymer. Triphenyl sulfonium triflate PAG was loaded at 5 wt % relative to the polymer except for LUVR-99474; LUVR-99474 has an identical formulation to LUVR-99494 except that the PAG used was t-butyl diphenyl iodonium nonaflate.

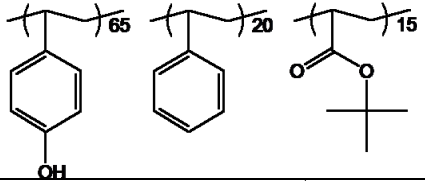
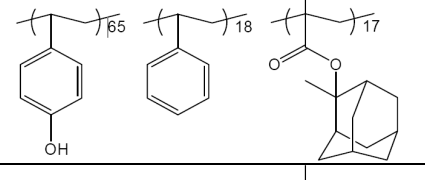
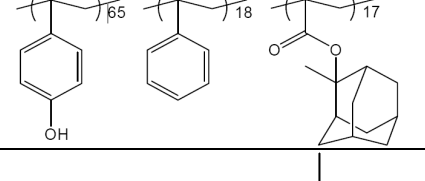
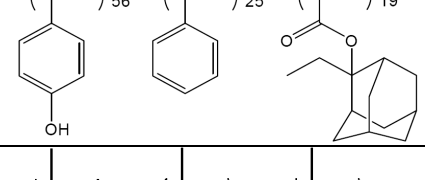
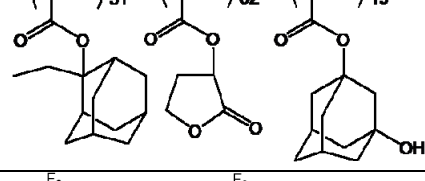
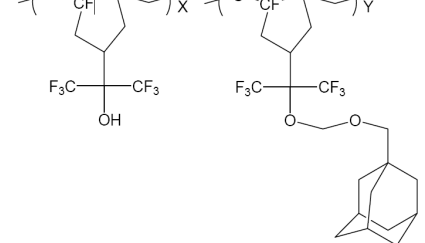
Resist Code	Resist Name	Polymer	Polymer Structure
PS(M)-2	LUVR-99497	Poly-J 65:20:15 HOST:ST:TBA	
PS-Acrylate(M)-3	LUVR-99474	Poly-JM 65:18:17 HOST:ST:MAAdMA	
PS-Acrylate(M)-4	LUVR-99494	Poly-JM 65:18:17 HOST:ST:MAAdMA	
PS-Acrylate(M)-7	LUVR-99496	Poly-JE 56:25:19 HOST:ST:EAdMA	
Acrylate(M)-2	LUVR-99495	Poly-A3 31:52:19 EAdMA:GBLMA:HAdMA	
F-Acrylate(M)-1	LUVR-99498	Poly-F4 60:40: FUGU:FUGU-AdMOM	

Table 2 – The polymers used in the six model resist formulations. They are comprised of the monomers hydroxystyrene (HOST), styrene (ST), t-butyl acrylate (TBA), methyl adamantyl methacrylate (MAAdMA), ethyl adamantyl methacrylate (EAdMA), γ -butyrolactone methacrylate (GBLMA), adamantylmethoxymethyl (AdMOM), FUGU, and FUGU-AdMA.

2.2 Processing

All resists were spun to a thickness of 60 nm on BARC-coated wafers, except for the EUV wafers which were bare Si with a hexamethyldisilazane (HMDS) treatment. The 157 nm and 193 nm exposures used 4" wafers, the 248 nm wafers were 6", the Intel EUV wafers were 12", and the remaining wafers were 8". Simulations were performed for each wavelength over a range of typical n & k values to find an optimal BARC thickness which minimized the negative effects of substrate reflection on the intensity profile (see Figure 1). The BARC i-CON-16 from Brewer Science was used at 590 nm thickness for the 299 nm exposures. Brewer Science BARC DUV-46 was used at 162 nm thickness for

the 265 nm exposures and 165 nm thickness for the 232 nm exposures. Rohm and Haas BARC AR3 at 62 nm thickness was used for both the 157 nm and 248 nm exposures. ARC29A from Brewer Science was used at a thickness of 79 nm for the 193 nm exposures.

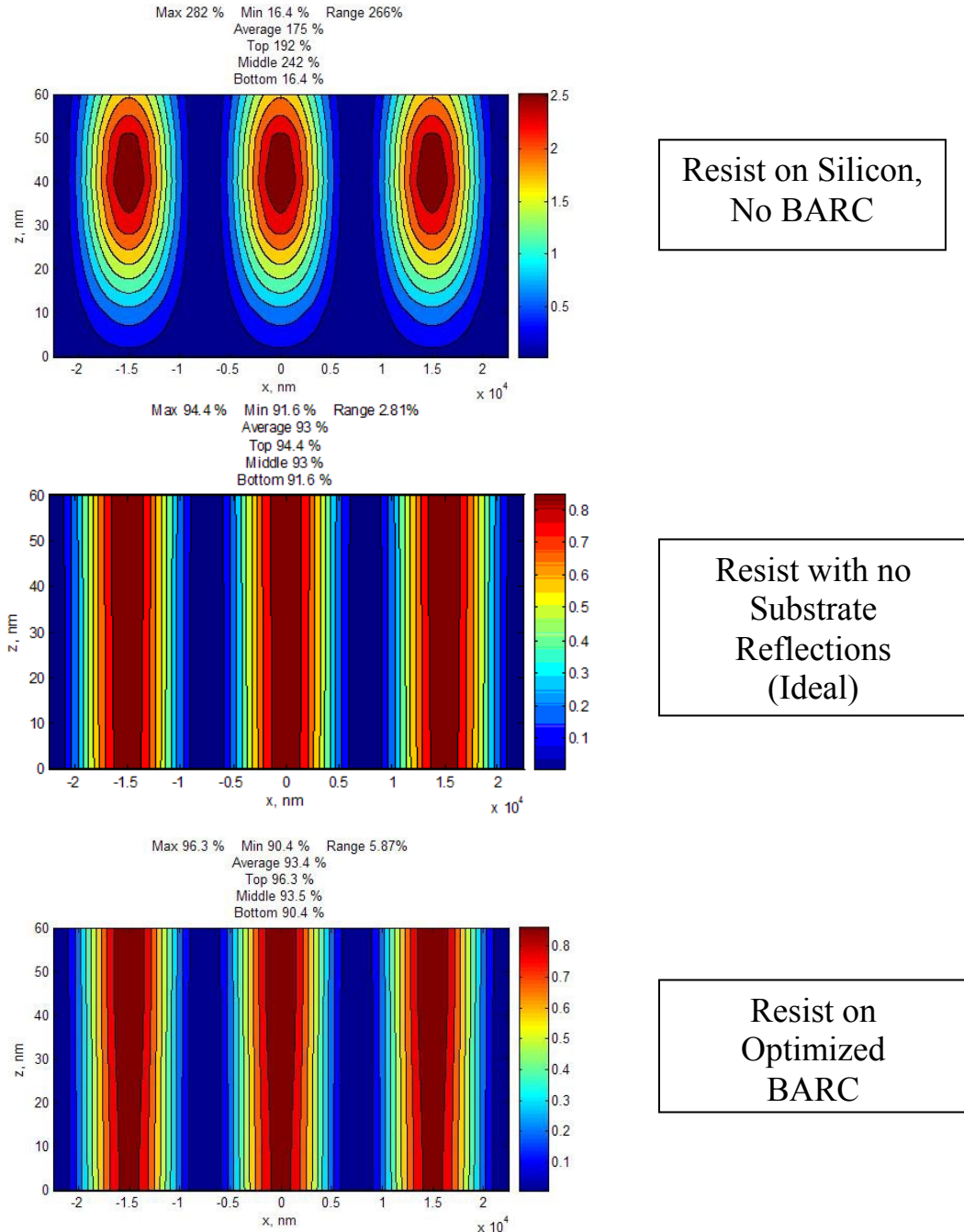


Figure 1 – Simulations of resist cross sections under 300 nm exposure where z is perpendicular to the wafer and the color denotes the relative intensity compared to that with no substrate reflections. The top profile is for a typical resist exposed with no BARC; there is little intensity near the substrate and the average intensity is nearly doubled what it would be if there were no substrate reflection. The middle profile shows the expected intensity if there were no substrate reflections. The bottom profile is the intensity with an optimized BARC. For some wavelengths the profile shape with the BARC did not match the ideal profile, but the maximum, minimum, and average intensities were reasonably well matched to the ideal profile.

The processing conditions for the model resists were a post-apply bake (PAB) of 130°C/60s, a post-expose bake (PEB) of 130°C/90s, and a 20s develop in 2.38% tetramethylammonium hydroxide (TMAH). The commercial resists processing conditions varied with resist, with a PAB from 110°C - 130°C for 60 - 90s, a PEB from 110°C - 130°C for 60 - 90s, and a 48s develop in 2.38% TMAH (except the MIT-LL exposures used their standard 20s develop recipe).

2.3 Exposure

The 232 nm, 265 nm, 299 nm, 336 nm, and 365 nm exposures were performed at Intel using a HgXe lamp and wavelength filters which have a 50% bandwidth of approximately 10 nm. The lamp was a Newport Oriol® Flood Exposure Housing (model 92511) with a Digital Exposure Control (DEC) unit (model 68945) and a 1 kW HgXe bulb. The DEC was calibrated at each wavelength using a Coherent PS-10 Thermopile Sensor. The 157 nm, 193 nm, and 248 nm exposures were performed at Lincoln Laboratories. The 157 nm and 193 nm exposures used a laboratory-class projection system employing F₂ and ArF lasers respectively. The 248 nm exposures were performed with a Canon EX-4 248-nm 0.6 NA stepper employing a KrF laser. The EUV exposures at 13.5 nm were performed on Exitech Micro-exposure tools equipped with a 180 nm silicon membrane spectral purity filter to block the DUV wavelengths; the model polymers were exposed at Sematech in Albany, NY and the commercial polymers at Intel in Hillsboro, OR². The commercial resists were exposed at all of the above wavelengths. The model resists were only exposed at Sematech and MIT-LL (13.5 nm, 157 nm, 193 nm, and 248 nm).

To extract a clearing dose (E_0) standard contrast curve wafers were processed which consisted of open-field exposures with doses ranging from 0 mJcm⁻² to doses above the clearing dose. To minimize substrate effects, E_0 was calculated by fitting all of the thickness vs. dose points between 14% to 80% thickness loss (relative to the non-exposed thickness) and extrapolating to zero thickness.

2.4 Transmission and n & k measurements

For the commercial resists, the film transmission (T%) was measured from 190-700 nm on a J. A. Woollam UV-VIS spectrometer after coating 3" quartz wafers with the resist and baking at the appropriate PAB condition. The film thickness (t) was measured on 4" silicon wafers which were processed in the same manner as the quartz transmission samples. The absorbance (base 10) was calculated using Equation 1

$$\text{Equation 1} \quad Abs. = \frac{-\log(T\%)}{t}$$

The uncertainty in the thickness is about 7 nm owing to a within-wafer thickness variation of about 5 nm and a wafer-to-wafer thickness variation of 5 nm; this factor leads to a relative uncertainty in the absorbance value of approximately 9%. For all of the resists the index of refraction and extinction coefficient (n & k) were measured from 150 - 820 nm using a J. A. Woollam VUV-VIS spectrometer and the absorbance calculated using Equation 2,

$$\text{Equation 2} \quad Abs. = \frac{4\pi k}{2.3t}$$

The percent difference between the two methods (where available) was relatively low and exceeded 27% only when the absolute difference was < 0.3 μm⁻¹. The absorbance derived from k was used in the plots presented in this paper.

3. RESULTS AND DISCUSSION

Figure 2 displays the wavelength trend of the clearing dose (E_0) for each resist relative to the clearing dose at EUV. (We believe that the outlier at 232 nm for PS-Acrylate(C)-8 is an artifact of a degraded material sample.) The resists did not clear at 336 nm or 365 nm for applied doses up to 300 mJcm⁻²; this is expected since the resists were found to be transparent above 300 nm, such that few photons are absorbed resulting in no discernable photoactivity. All of the resists are very slow when exposed to 299 nm (from 4x to 40x slower than at EUV) owing to the relatively low absorption at that wavelength. The resists sensitivities at 248 - 265 nm are comparable to those at EUV with E_0 values ranging from 1/2 to 2.6x that at EUV. The resists tend to be more sensitive to light between 157 nm and 232 than to EUV, up to 13x faster

(excluding the single outlier which appears to be much faster). We define an envelope encompassing the fastest resists (relative to EUV) illustrated by the dashed line in Figure 2; the inverse of this envelope is shown in Figure 3.

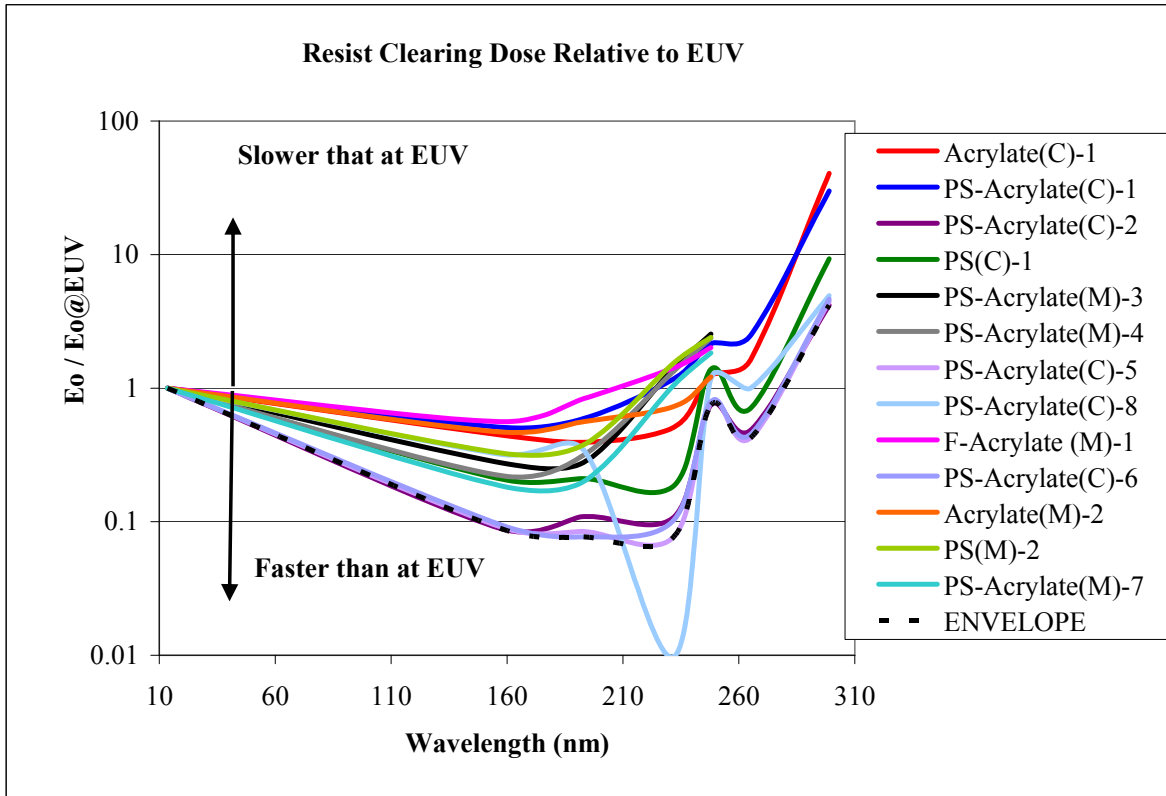


Figure 2 – The clearing dose (E_0) of each resist relative to that at EUV for exposure wavelengths from 13.5 to 299 nm. In the legend, (C) denotes resists provided by commercial suppliers and (M) denotes the model resists formulated at MIT-LL. The envelope encompassing the worst-case data points is shown as the dashed line.

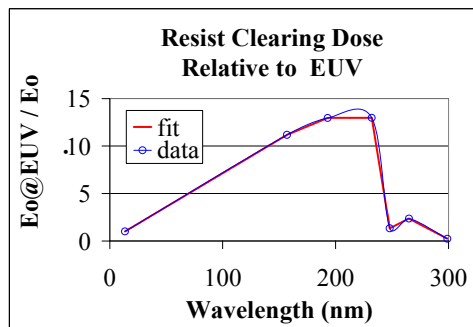


Figure 3 – The envelope encompassing the fastest resists relative to EUV, with a linear interpolation (red line) between each set of 2 data points. The data is inverted from that displayed in Figure 2.

The correlation between the clearing dose and absorbance is highlighted in Figure 4 - Figure 6. The overall trend, for a resist thickness of 60 nm, is that increased absorbance correlates with increased sensitivity. For resists with absorbance values which are approximately the same order of magnitude, the sensitivity is determined by more subtle resist characteristics such as PAG and base loadings, the protecting group, monomer ratios, and side reactions (such as cross-linking and chain scission).

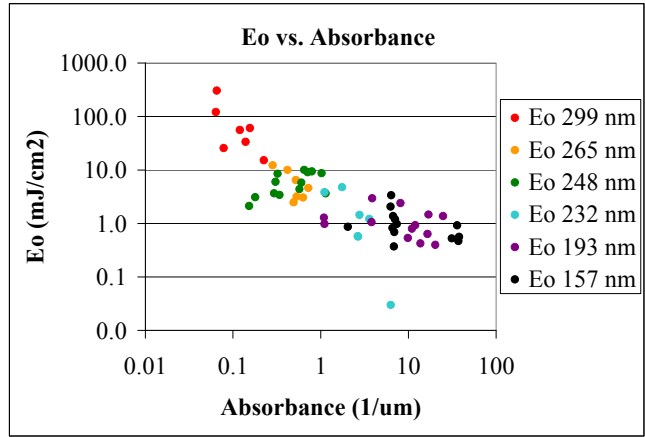


Figure 4 – The clearing dose (E_0) vs. absorbance (base 10) for all of the resists exposed at the VUV-VIS wavelengths.

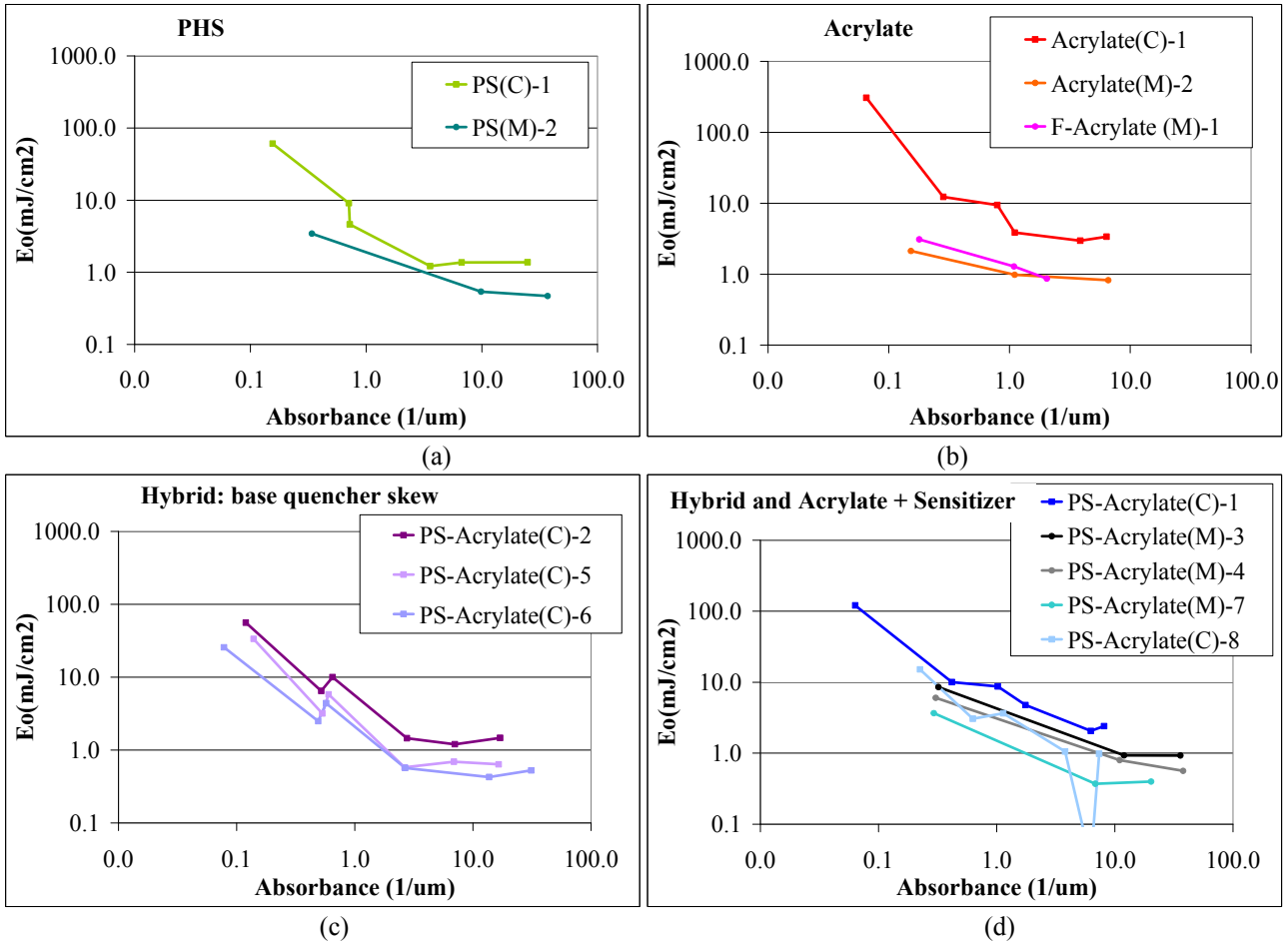


Figure 5 – The clearing dose (E_0) vs. absorbance at optical wavelengths (157 nm – 299 nm) for (a) the PS-type resists with polymers developed for 248 nm lithography, (b) acrylate-type resists with polymers developed for 193 nm and 157 nm lithographies, (c) a base quencher skew on a PHS-acrylate hybrid resist, and (d) the remaining hybrid resists as well as the acrylate resists with EUV sensitizers. For each class of materials the commercial resists tend to be slower than the model resists, possibly owing to the addition of stronger base quenchers in the commercial formulations which presumably gives rise to improved resolution.

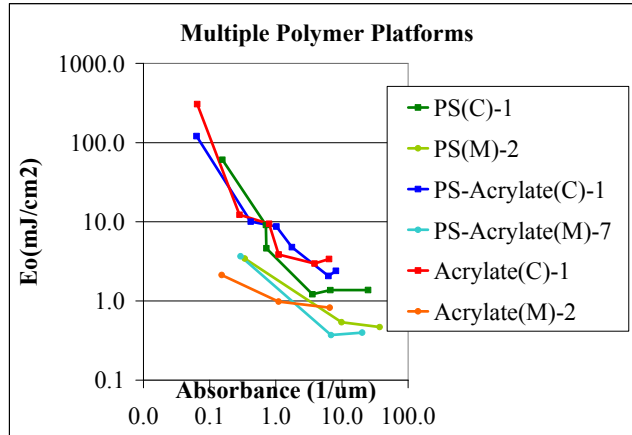


Figure 6 – A subset of the data from Figure 5 in which both the fastest and slowest resists of each class are plotted. The trends are similar for each resist with no clear differentiation based on polymer type, other than at the higher absorbance values ($4.0 - 6.5 \mu\text{m}^{-1}$) one might expect the two acrylate resists to be faster based on the trends of the other resists.

4. ADDITIONAL ANALYSIS

To assess the impact of resist sensitivity, we couple the worst case resist sensitivity curve (relative to EUV) with expected source output and mirror reflectivity data. The actual spectral output of the source depends on the type of source, the operating conditions, and the configuration⁷⁻¹⁰. Data representing one typical source spectral output is presented in Figure 7; the data were generated assuming a blackbody radiator at a temperature of 10 eV using Equation 3, consistent with Namba et al. for a Sn laser-produced plasma source⁸.

Equation 3

$$P = \frac{2\pi hc^2}{\lambda^5 e \left(\frac{hc}{kT\lambda} - 1 \right)}$$

Some data show that the amount of OOB radiation produced in the range 140 – 400 nm is approximately 10 - 20% of the in-band radiation at 13.5 nm with a 2% bandwidth; other data estimate the DUV-IR power to be 30-70% of the in-band power¹⁶⁻¹⁹. For this example we assume the OOB power to be 20% of the in-band power and assume a flat spectral distribution near EUV. The assumption of a flat spectral distribution is of little consequence because the EUV bandwidth is only 0.27 nm.

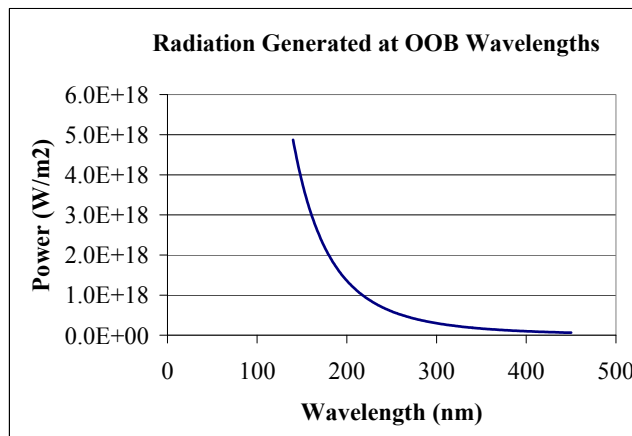


Figure 7 – The power distribution of an EUV plasma source in the range 140 – 450 nm assuming a black body radiator at a temperature of 10 eV. The scale was normalized assuming the power into 140 – 450 nm is 20% of the power into 13.5 nm with a 2% bandwidth.

For the OOB optic reflectivity we use reflectance data measured on a standard Ru-coated EUV mask, displayed in Figure 8(a). We assume that this reflectivity applies to each of the mirrors in the system. The actual reflectivity of the mirrors depends on several factors including the details of the multilayer capping layer (both the thicknesses and material). For this example we assume an 11 mirror system and raise the single mirror reflectivity to the 11th power as displayed in Figure 8(b). The number of mirrors that will be used on an actual manufacturing tool will likely be different. The reflectivity of a typical MLC mask near 13.5 nm is shown in Figure 9.

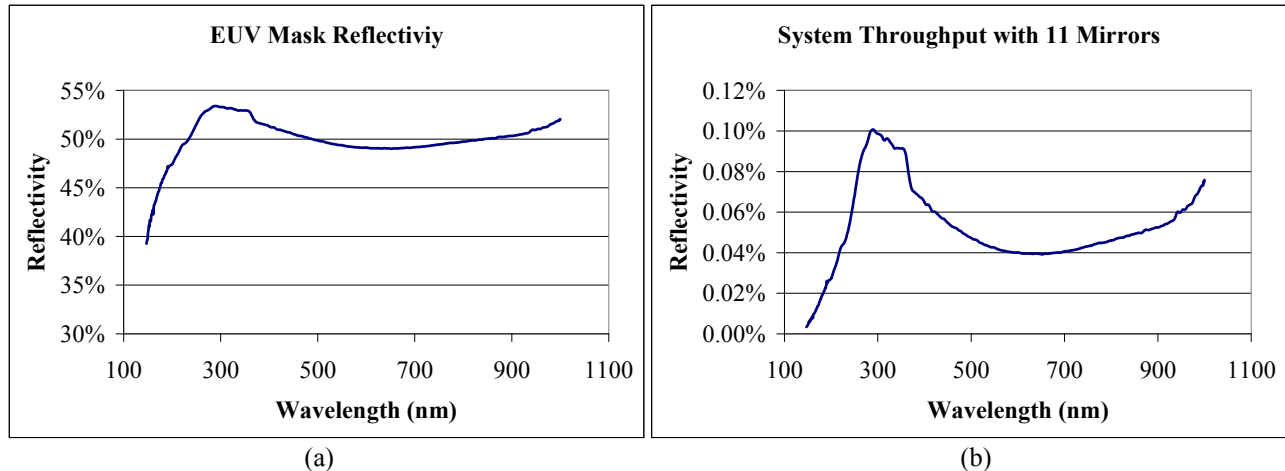


Figure 8 – (a) The reflectivity in the wavelength range 115 – 1000 nm for a typical Ru-coated multilayer mask. The data above 190 nm were measured at Intel on an n & k analyzer and the data below that are based on modeling. (b) The expected system throughput obtained by assuming an 11 mirror system with each mirror having the reflectivity profile shown in (a).

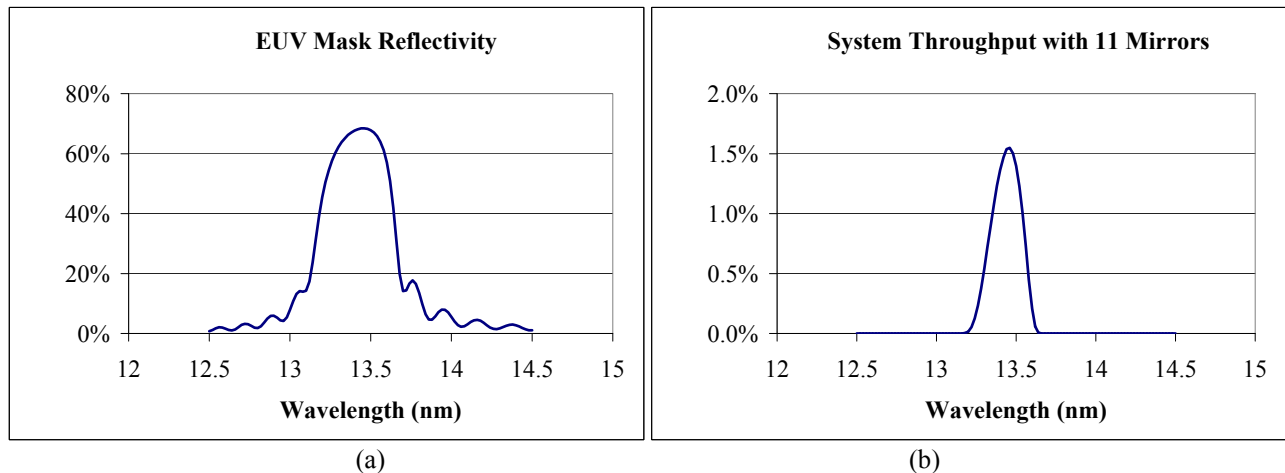


Figure 9 – (a) The spectral reflectivity in the wavelength region near 13.5 nm for a Ru capped multilayer (provided courtesy of NIST) and (b) the expected system throughput obtained by assuming an 11 mirror system with each mirror having the reflectivity profile shown in (a).

Combining the data presented in Figure 7 - Figure 9 provides an estimate for the spectral power distribution at the wafer plane (Figure 10). This would result in the OOB power delivered to the wafer plane being 0.5% of the in-band power. This result can change by over 2 orders of magnitude by changing the input data, including the source spectral output, the mirror reflectivity, and the number of mirrors.

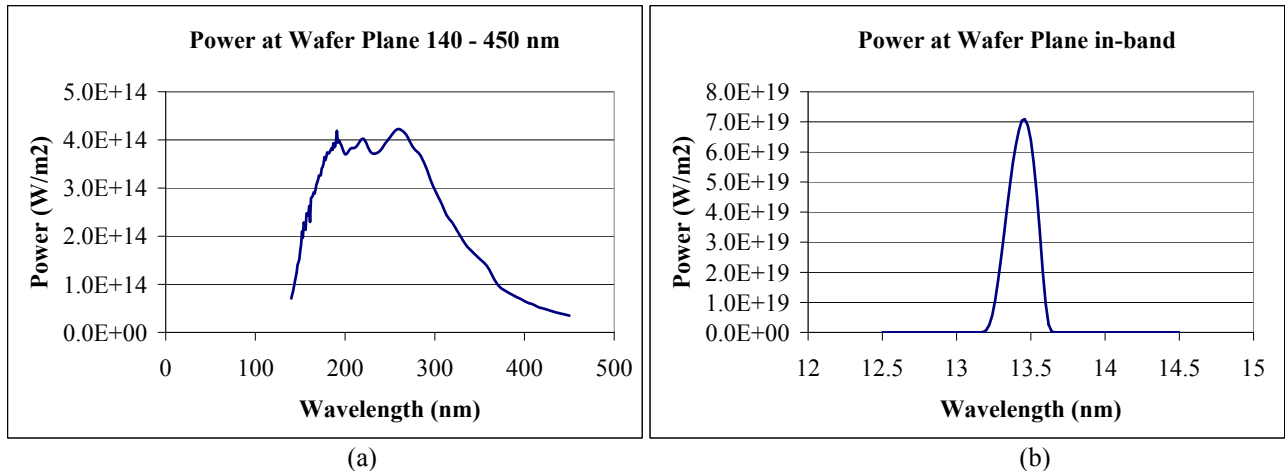


Figure 10 – The expected power arriving at the wafer plane for (a) the OOB range 140 – 450 nm and (b) the in-band power.

To estimate the effect this OOB power has on the resist we use the envelope encompassing the fastest resists (relative to EUV) presented in Figure 3. Although this is a reasonable assumption based on available data, not all possible resists have been explored and new resists will likely be developed which may shift the envelope. Multiplying the relative resist envelope by the OOB power reaching the wafer plane (relative to in-band power) yields the data shown in Figure 11. The resulting impact of OOB radiation incident on the resist would be 2.6% of the in-band; this was calculated by taking the area under the curve in Figure 11 (0.007) and dividing it by the relative EUV power (0.27). The data suggests that the primary OOB region of concern for maximizing resist contrast is 160 – 240 nm (FWHF) and to a lesser extent the wavelength range 140 – 300 nm. Below 160 nm the system reflectivity drops dramatically based on the data in Figure 8. Above 240 nm the source output power quickly reduces based on the data in Figure 7. Also, the resists start to become insensitive somewhere between 265 – 299 nm.

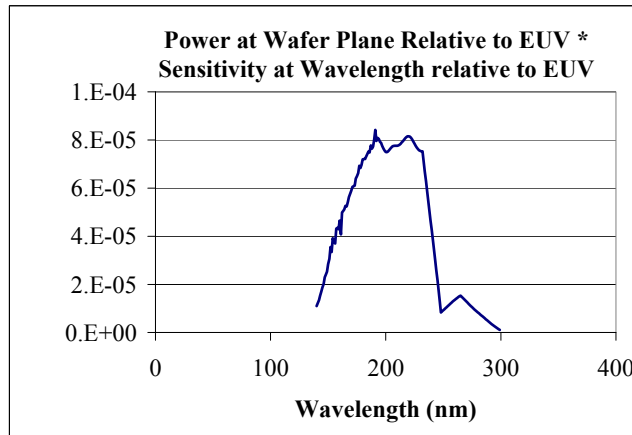


Figure 11 – The OOB sensitivity of resists relative to EUV multiplied by the relative OOB power at the wafer plane relative to EUV. This illustrates that the main wavelengths of concern are between 160 – 240 nm.

To demonstrate how the system parameters can change the results, the OOB reflectivity for various capping layers is shown in Figure 12(a) (data provided by Fraunhofer Institute, IOF, Jena)^{20,21}. The resulting affect in resist is displayed in Figure 12(b).

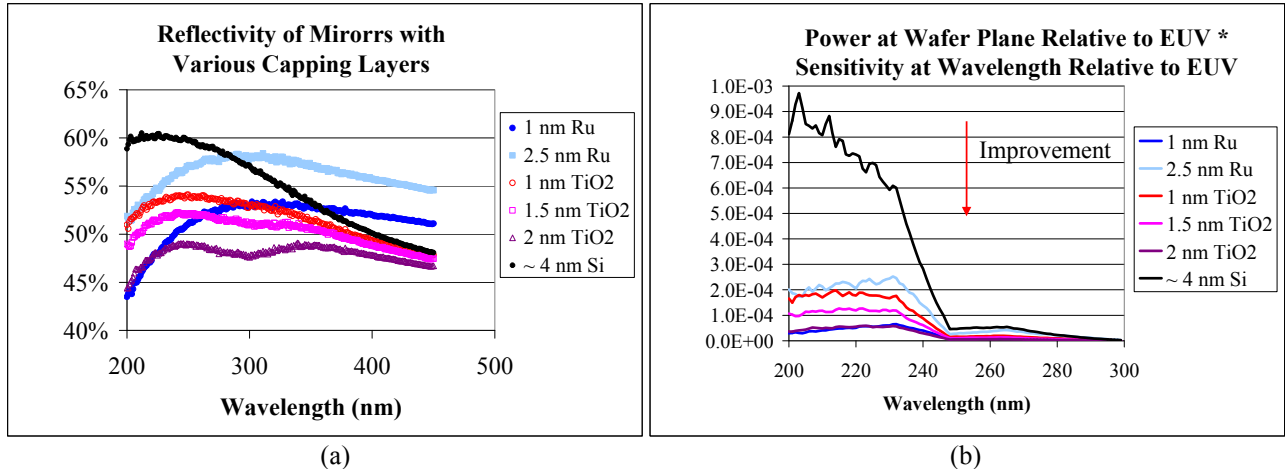


Figure 12 – (a) The MLC reflectivity for various capping layers (provided by Fraunhofer Institute, IOF, Jena) and (b) the resulting impact in resist at the wafer plane. Although the 1 nm Ru and 2 nm TiO₂ capping layers diverge on the reflectivity plot, the expected impact in resist is nearly identical.

5. DISCUSSION AND CONCLUSIONS

The relative sensitivity of EUV resists to out of band radiation in the spectral range 157 - 400 nm was measured for 13 EUV resists spanning a wide range of resist platforms and formulations. We found that many of the general trends identified by Mbanaso et al.⁵ apply to the expanded data set, specifically that for a given resist the sensitivity tracks with absorbance, that resist sensitivity decreases dramatically for wavelengths approaching 300 nm, and that sensitivity is negligible for longer wavelengths (which is expected owing to the low absorbance at the higher wavelengths). We also found that for resists with absorbance values on the same order of magnitude, the resist sensitivity is determined by other aspects of the resist formulation (such as the protecting group, PAG, and base quencher). However, one can reasonably estimate the OOB sensitivity of the resists measured (to within about an order of magnitude) in the measured wavelength range using resist absorbance values. Within the wavelength region explored the greatest concern is near 160 – 240 nm based on current resist sensitivity characteristics.

However, one must be careful interpolating the data between 13.5 - 157 nm. Under EUV exposure PAGs are predominately activated by secondary electrons. The secondary electron yield (SEY) in resist increases with decreasing wavelength²². There is a gap in resist sensitivity data in the wavelength region 13.5 – 157 nm. Furthermore, other concerns may motivate modifying the source spectral profile. For example, data suggests that lower wavelengths contribute disproportionately to the rate of contamination accumulation on EUV mirrors²³.

There are several options for reducing the amount of OOB radiation incident on the wafer plane. Mirror coatings could be tuned by varying material and thickness to change the spectral reflectivity characteristics^{21, 24}. A thin membrane spectral purity filter could be implemented,^{19, 25} or a diffraction grating could be used to filter unwanted wavelengths. However, each potential solution will have some impact on the in-band throughput so any solution should take into account the potential impact in resist

ACKNOWLEDGEMENTS

The authors thank Emil Piscani and the rest of the Sematech team in Albany for EUV exposures and collecting n & k data. We thank Sergiy Yulin and the rest of the team at the Fraunhofer Institute, IOF, Jena, for providing the reflectivity data on various capping layers and allowing us to publish it. We thank Simi A. George for providing EUV source data that she extracted from the published literature. We thank Guojing Zhang for measuring and providing mask reflectivity data. We acknowledge the MEL lithography team at Lincoln Laboratory for performing some of the lithography. We thank Michael Sheehan and Matt Romberger at DuPont Electronic Polymers for providing materials used in this study. We thank Steve Dawson at Brewer Science and Steve Putna at Intel for assistance in selecting a BARC as well as providing the material.

The Lincoln Laboratory portion of this work was sponsored by a Cooperative Research and Development Agreement between Lincoln Laboratory and Intel Corporation. Opinions, interpretations, conclusions, and recommendations are those of the authors and are not necessarily endorsed by the United States Government.

REFERENCES

- [1] [Http://Www.Itrs.Net/](http://www.itrs.net/).
- [2] Roberts, J., Bacuita, T., Bristol, R. L., Cao, H., Chandhok, M., Lee, S. H., Leeson, M., Liang, T., Panning, E., Rice, B. J., Shah, U., Shell, M., Yueh, W., and Zhang, G., "Exposing extreme ultraviolet lithography at Intel," *Microelectronic Engineering*, **83**(4-9), 672-675 (2006).
- [3] Putna, E. S., Younkin, T. R., Chandhok, M., and Frasure, K., "EUV Lithography for 30nm Half Pitch and Beyond: Exploring Resolution, Sensitivity and LWR Tradeoffs," *Proceedings of the SPIE - The International Society for Optical Engineering* 7273-110, (2009).
- [4] Cao, H., Bristol, R., Yueh, W., Chandhok, M., and Kaplan, S., "EUV Resist Sensitivity to Out of Band (OOB) Radiation," presented at the 3rd International EUVL Symposium, Miyazaki, Japan, November 1-4, (2004).
- [5] Mbanaso, C., Denbeaux, G., Dean, K., Brainard, R., Kruger, S., and Hassanein, E., "Investigation of sensitivity of extreme ultraviolet resists to out-of-band radiation," *Emerging Lithographic Technologies XII* **6921**, 69213L-69219 (2008).
- [6] George, S. A., Naulleau, P. P., Rekawa, S., and Kemp, D., "DUV source integration into the 0.3 NA Berkeley SEMATECH MET for OOB exposure studies," presented at the 2008 International Symposium on Extreme Ultraviolet Lithography Lake Tahoe, California, September 28 - October 1, (2008).
- [7] Sakaguchi, H., Fujioka, S., Namba, S., Tanuma, H., Ohashi, H., Suda, S., Shimomura, M., Nakai, Y., Kimura, Y., Yasuda, Y., Nishimura, H., Norimatsu, T., Sunahara, A., Nishihara, K., Miyanaga, N., Izawa, Y., and Mima, K., "Absolute evaluation of out-of-band radiation from laser-produced tin plasmas for extreme ultraviolet lithography," *Applied Physics Letters* **92**(11), 111503-111503 (2008).
- [8] Namba, S., Fujioka, S., Sakaguchi, H., Nishimura, H., Yasuda, Y., Nagai, K., Miyanaga, N., Izawa, Y., Mima, K., Sato, K., and Takiyama, K., "Characterization of out-of-band radiation and plasma parameters in laser-produced Sn plasmas for extreme ultraviolet lithography light sources," *Journal of Applied Physics* **104**(1), 013305-013305 (2008).
- [9] Morris, O., Hayden, P., O'reilly, F., Murphy, N., Dunne, P., and Bakshi, V., "Angle-resolved absolute out-of-band radiation studies of a tin-based laser-produced plasma source," *Applied Physics Letters* **91**(8), 081506-081503 (2007).
- [10] Komori, H., Ueno, Y., Hoshino, H., Ariga, T., Soumagne, G., Endo, A., and Mizoguchi, H., "EUV radiation characteristics of a CO2 laser produced Xe plasma," *Applied Physics B: Lasers and Optics* **83**(2), 213-218 (2006).
- [11] Kozawa, T., Tagawa, S., Cao, H. B., Deng, H., and Leeson, M. J., "Acid distribution in chemically amplified extreme ultraviolet resist," *Journal of Vacuum Science and Technology B* **25**, 2481-2485 (2007).
- [12] Roberts, J. M., Meagley, R., Fedynyshyn, T. H., Sinta, R. F., Astolfi, D. K., Goodman, R. B., and Cabral, A., "Contributions to innate material roughness in resist," *Advances in Resist Technology and Processing XXIII* **6153**, 61533U-61511 (2006).
- [13] Fedynyshyn, T. H., Astolfi, D. K., Goodman, R. B., Cann, S., and Roberts, J., "Contributions of resist polymers to innate material roughness," *Journal of Vacuum Science and Technology B* **26**, 2281-2289 (2008).
- [14] Fedynyshyn, T. H., Goodman, R. B., and Roberts, J., "Polymer matrix effects on acid generation," *Advances in Resist Materials and Processing Technology XXV* **6923**, 692319-692312 (2008).
- [15] Fedynyshyn, T. H., Sinta, R. F., Astolfi, D. K., Goodman, R. B., Cabral, A., Roberts, J., and Meagley, R., "Resist deconstruction as a probe for innate material roughness," *Journal of Microlithography, Microfabrication, and Microsystems* **5**(4), 043010-043012 (2006).
- [16] George, S. A., personal communication, (2009).
- [17] Sematech, "Technology Transfer #04024490A-TR," (2004).
- [18] Van De Kruijs, R. W. E., Yakshin, A. E., Van Herpen, M. M. J. W., Klunder, D. J. W., Louis, E., Van Der Westen, S. A., Enkisch, H., Mullender, S., Bakker, L., Banine, V., Richter, M., and Bijkerk, F., "Multilayer optics with spectral purity enhancing layers for the EUV wavelength range," presented at the 4th International EUVL Symposium and Source Workshop, San Diego, CA, November, (2005).

- [19] Banine, V., Yakunin, A., Salashchenko, N., Kluev, E., Lopatin, A., Luchin, V., Tsybin, N., Sjmaenok, L., Soer, W., and Jak, M., "Spectral Purity Filter Development for EUV HVM," presented at the 2008 International Symposium on Extreme Ultraviolet Lithography, Lake Tahoe, CA, September 28 - October 1, (2008).
- [20] Yulin, S., Schürmann, M. C., Nesterenko, V., Schürman, M., and Feigl, T., "Environmental stability of promising capping layers under high-power EUV pulsed source," unpublished (2008).
- [21] Yulin, S., Benoit, N., Feigl, T., Kaiser, N., Fang, M., and Chandhok, M., "Mo/Si multilayers with enhanced TiO₂- and RuO₂-capping layers," *Emerging Lithographic Technologies XII* **6921**, 692118-692110 (2008).
- [22] Bartynski, R. A., Yakshinskiy, B. V., and Madey, T. E., "Study of photoresist samples by secondary electron yield " unpublished (2008).
- [23] Denbeaux, G., Fan, Y.-J., Alin, A., Yankulin, L., Garg, R., Wood, O., Goodwin, F., Koay, C.-S., Gullikson, E. M., Goldberg, K. A., Anderson, E., and Chao, W., "Actinic microscope for EUV masks using a stand-alone source for imaging and contamination studies of EUV masks," presented at the 2007 International EUVL Symposium, Sapporo, Japan, 28-31 October, (2007).
- [24] Louis, E., Van De Kruijs, R. W. E., Yakshin, A. E., Van Der Westen, S. A., Bijkerk, F., Van Herpen, M. M. J. W., Klunder, D. J. W., Bakker, L., Enkisch, H., Mullender, S., Richter, M., and Banine, V., "Multilayer optics with spectral purity layers for the EUV wavelength range," *Emerging Lithographic Technologies X* **6151**, 615139-615135 (2006).
- [25] Powell, F. R. and Johnson, T. A., "Filter windows for EUV lithography," *Emerging Lithographic Technologies V* **4343**, 585-589 (2001).